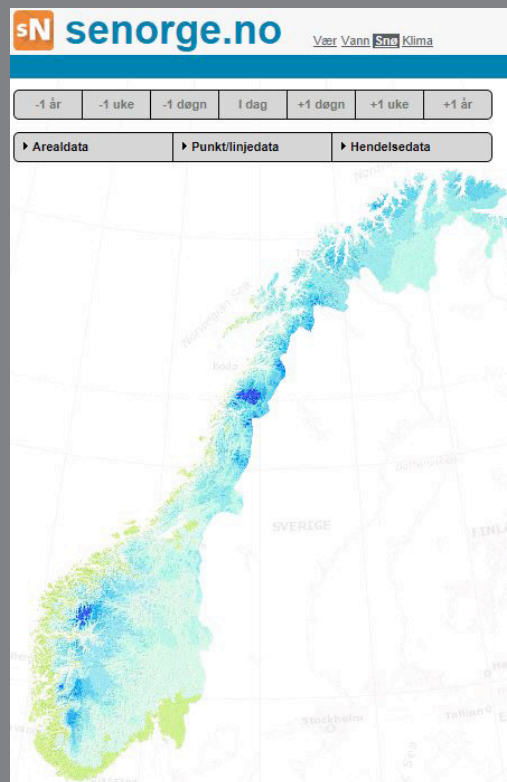




New version (v.1.1.1) of the seNorge snow model and snow maps for Norway

Tuomo Saloranta

6
2014



R
A
P
P
O
R
T

New version (v.1.1.1) of the seNorge snow model and snow maps for Norway

Report no. 6 – 2014

New version (v.1.1.1) of the seNorge snow model and snow maps for Norway

Published by: Norwegian Water Resources and Energy Directorate

Authors: Tuomo Saloranta

Cover photo: seNorge.no

Published: Web

ISSN: 1501-2832

ISBN: 978-82-410-0951-8

Abstract: In order to enhance the accuracy and precision of the snow maps, and to remove the detected significant systematic biases, a new revised version (v.1.1.1) of the seNorge snow model was developed during 2012-2013. This report summarizes the revisions made to the new seNorge snow model (v.1.1.1), and describes in some more details the development of the new snow melt module, based on statistical analysis of NVEs snow pillow data, as well as the new addition to the model for estimation of the snow distribution and fraction of snow-covered area in the model grid cells.

Key words: seNorge; snow; modelling

Norwegian Water Resources and Energy Directorate
Middelthunsgate 29
P.O. Box 5091 Majorstua
N 0301 OSLO
NORWAY

Telephone: +47 22 95 95 95

Fax: +47 22 95 90 00

E-mail: nve@nve.no

Internet: www.nve.no

January 2014

Contents

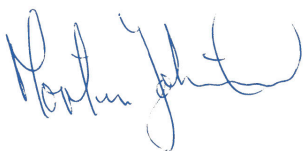
Preface	4
Summary	5
1 Introduction	6
2 The seNorge snow model v.1.1.1: What is new?	7
2.1 Main new features	7
2.1.1 Snow melt season.....	7
2.1.2 Snow accumulation season.....	7
2.1.3 Fraction of snow-covered area in model grid cells.....	7
2.2 Did the snow maps get any better?.....	8
2.2.1 Discussion	9
2.3 Revised seNorge snow model (v.1.1.1) parameter values	10
3 Daily snow melt rates in Norway: observations and modelling	12
3.1 Data and Methods	12
3.1.1 Data description	12
3.1.2 The previous (v.1.1) seNorge snow melt algorithm	15
3.2 Results.....	16
3.2.1 The new revised seNorge (v.1.1.1) snow melt algorithm	16
3.2.2 “Extreme value” models	21
3.3 Summary	21
4 New algorithm for subgrid snow distribution and fraction of snow-covered area in the seNorge snow model.	23
4.1 Introduction	23
4.2 The algorithm description.....	23
4.2.1 Appendix: Details behind Equation 6b.....	28
5 Conclusions	29
Acknowledgements	29
References	29

Preface

Good information of snow conditions is important for many of the NVEs areas of work, such as hydropower production planning and forecasting of floods, slush flows and avalanche danger levels. The national snow maps simulated by the seNorge model are often the main source of daily updated regional snow information.

In order to enhance the accuracy and precision of the snow maps, and to remove the detected significant systematic biases, an NVE Research & Development project was conducted in 2012-2013. The main outcome from this project was the new revised version (v.1.1.1) of the seNorge snow model. The operational version of this model was constructed by Jess Andersen at the NVEs section for Hydroinformatics. This report summarizes the revisions made to the new seNorge snow model (v.1.1.1), which has since autumn 2013 been producing a new set of more accurate snow maps, extending all the way from 1957 to the present (and even 9 days in the future).

Oslo, January 2014



Morten Johnsrud

Director



Rune Engeset
Head of Section

Summary

To be able to better meet demands on providing updated detailed information on regional snow conditions in Norway, national snow maps have been produced at the Norwegian Water Resources and Energy Directorate (NVE) with the seNorge snow model since 2004, in co-operation with the Norwegian Meteorological Institute (MET).

In order to enhance the accuracy and precision of the snow maps, and to remove the detected significant systematic biases, a new revised version (v.1.1.1) of the seNorge snow model was developed during 2012-2013. The model parameters were optimized by using Markov chain Monte Carlo (MCMC) simulation and historical snow data from the NVEs snow pillows, as well as from the snow course measurements of the hydropower companies.

This report summarizes the revisions made to the new seNorge snow model (v.1.1.1), and describes in some more details the development of the new snow melt module, based on statistical analysis of NVEs snow pillow data, as well as the new addition to the model for estimation of the snow distribution and fraction of snow-covered area in the model grid cells.

The evaluation of the new revised snow model (v.1.1.1) shows that the significant biases detected in the previous model version are removed, and the Nash-Sutcliffe model performance indicator has increased from the negative values of -0.54 and -1.70 for snow water equivalent and density, respectively, to the clearly positive values of 0.61 and 0.30. Comparison with snow depth data from meteorological stations show, among others, that the percentage of “good match” station in the spring (end of April) has increased from 42 % (v.1.1) to 65 % (v.1.1.1).

1 Introduction

A significant fraction of the annual precipitation in Norway (approximately 30 %) falls as snow. Snow plays an important role in, among others, hydropower production planning, forecasting of floods, slush flows and avalanche danger levels. Snow is a prerequisite for many winter sport activities, and a challenge for construction safety and for traffic flow at airports and on roads and railways. Snow cover is also a key factor in the weather and climate system, both regionally and globally.

To be able to better meet demands on providing updated detailed information on regional snow conditions in Norway, national snow maps have been produced at the Norwegian Water Resources and Energy Directorate (NVE) with the seNorge snow model since 2004 (Tveito et al. 2002, Engeset et al. 2004a, Engeset et al. 2004b; Saloranta, 2012), in co-operation with the Norwegian Meteorological Institute (MET) and the Norwegian Mapping Authority. Since snow conditions vary strongly with the date of the snow season, region, elevation, and the type of winter (e.g. cold and dry vs. wet and warm winters, depending on the type of the large scale atmospheric circulation patterns), models at small enough spatiotemporal resolution are indeed needed to resolve the rather high variability in snow conditions in the mountainous Norway.

The seNorge snow model evaluation studies (Engeset et al., 2004b; Stranden, 2010; Dyrørdal, 2010; Saloranta, 2012) have pointed out some significant systematic biases in the simulated snow conditions. The statistical evaluation of the seNorge model by Saloranta (2012) compared the model simulations against two large datasets from the hydropower companies and MET, and confirmed the previous evaluation results on that the seNorge model generally overestimates the snow water equivalent (*SWE*) and snow bulk density (ρ). Moreover, the distribution of model fit for *SWE* in Saloranta (2012) showed a clear dependency on elevation throughout the snow season. E.g., around the end of March, the model overestimated *SWE* on average by +34 % in the 400-600 m a.s.l. elevation interval, while by as much as 100 % in the higher 1000-1200 m a.s.l. elevation interval. The seNorge model was found to overestimate also ρ on average by approximately 0.1 kg/L, but there was only a moderate variation in the model fit along the snow season and elevation for ρ . The R^2 -values in Saloranta (2012), however, indicated that the model performs rather well in simulating the observed variability in *SWE* and ρ , despite of the overestimation of absolute values. Due to the known systematic biases one has usually been bound to use relative snow conditions (e.g. comparisons of current *SWE* to a 30-year median *SWE*) instead of absolute values in practical applications. The lack of accurate absolute values of snow conditions has been a real limitation for many existing and potential new applications of the snow maps.

In order to enhance the accuracy and precision of the snow maps, and to remove the systematic biases, a new revised version (v.1.1.1) of the seNorge snow model was developed during 2012-2013. Furthermore, the model parameters were optimized by using Markov chain Monte Carlo (MCMC) simulation and historical snow data from the NVEs snow pillows, as well as from the snow course measurements of the hydropower companies.

This report summarizes the revisions made to the new seNorge snow model (v.1.1.1) , and describes in some more details the development of the new snow melt module as well as the new module for estimating the snow distribution and fraction of snow-covered area in the model grid cells.

2 The seNorge snow model v.1.1.1: What is new?

2.1 Main new features

2.1.1 Snow melt season

The melt algorithm in the new model version is revised on the basis of approximately 3350 observations of daily melt rate from NVEs snow pillow stations, spanning a variety of years, latitudes and elevations. In the revised model there is a new temperature-independent melt term in addition to the temperature-dependent degree-day term. This new term is proportional to the potential solar radiation, and varies thus with the combination of latitude and time of the year. For more details, see section 3.

2.1.2 Snow accumulation season

On the basis of 580 observations of *SWE* and snow density (ρ) from approximately 200 snow stations of the hydropower companies, spanning a variety of years, latitudes and elevations, the following adjustments are made to the revised model:

- The input snow precipitation is adjusted, depending on the model grid cell elevation. The reduction factor of input precipitation decreases gradually with elevation, the endpoints being so that below ~200 m a.s.l. no correction is made, and above ~700 m a.s.l. ~40 % of the input precipitation is removed. This input correction is justified due to uncertainties in precipitation lapse rate and catch correction of the precipitation measurements. Optimal value (with uncertainty range) of the correction parameter f_s is estimated in the MCMC simulation (piecewise linear correction on log-scale, involving three parameters; see section 2.3).
- The snow compaction and density routine is revised among others by introducing different new snow densities above and below the treeline (due to generally higher wind speeds above the treeline), by introducing increased compaction due to liquid water in the snowpack, and by removing the unnecessary “instant compaction step”. Optimal value (with uncertainty range) of the density-viscosity-relation parameter C_6 is estimated in the MCMC simulation (see section 2.3).

2.1.3 Fraction of snow-covered area in model grid cells

The distribution of snow and the fraction of snow-covered area (*SCA*) within the model 1x1 km grid cells are now simulated. This affects specifically snow melt rates when $SCA < 1$, by reducing the grid cell average melt rate and by lengthening the snow (melt) season. The uniform probability distribution $U(min, max)$ is assumed for snow within each grid cell, and the parameter values for the *SCA* model are based on high-resolution ground-penetrating snow-radar data from Hardangervidda as well as expert judgement. For more details, see section 4.

2.2 Did the snow maps get any better?

Yes, they did. Especially the *accuracy* got better, while the *precision* did not seemingly improve that much. A comparison of simulations against the 580 observations of *SWE* and ρ from approximately 200 stations of the hydropower companies (Figure 1) shows that the significant biases for *SWE* and ρ along elevation, simulated by the old (v.1.1) snow model, have been removed in the new revised version (v.1.1.1). The corresponding changes in the model performance indicators are listed in Table 1.

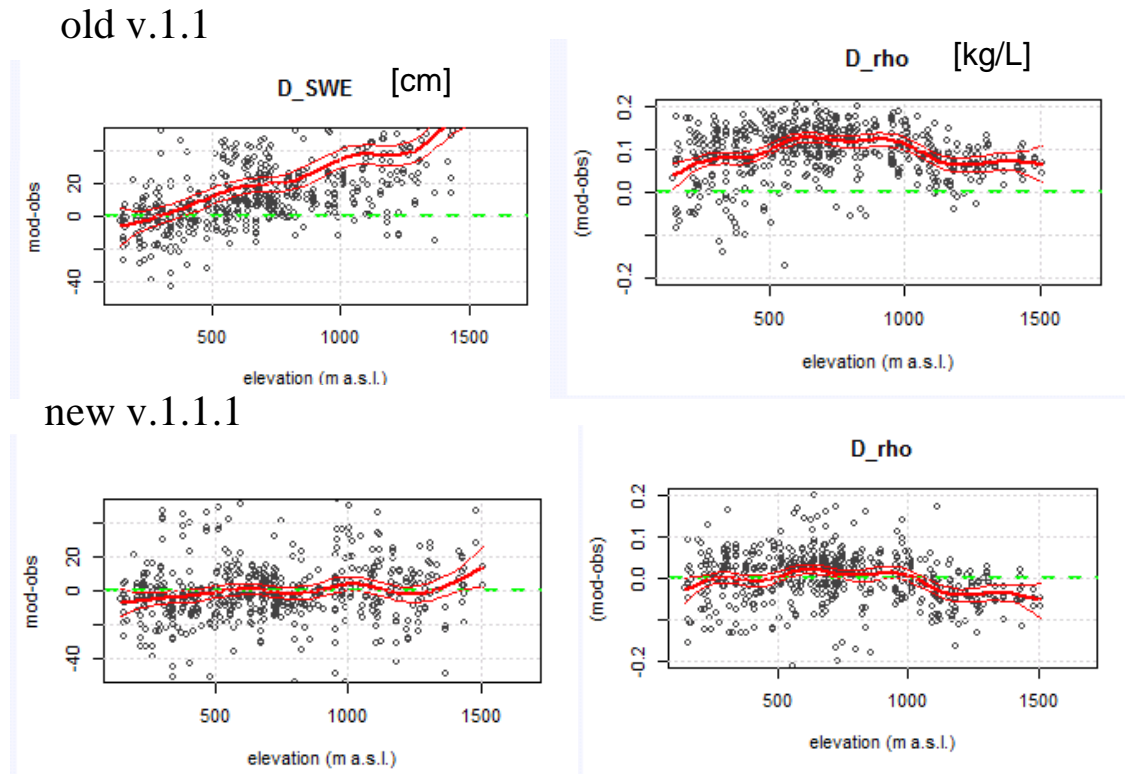


Figure 1. Difference between simulated (upper and lower panels show old and new model version, respectively) and observed *SWE* (NB! in units [cm]) and ρ [kg/L]. The 580 observations from ~200 stations of the hydropower companies are used in the comparison. The red line denotes a GAM-curve (with 2*S.E.) fitted to the cloud of points. Green dashed line shows the perfect 1:1 fit.

Table 1. Comparison of model performance indicators between the old (v.1.1) and the new revised versions (v.1.1.1) of the seNorge snow model.

	<i>SWE</i>			ρ		
	mean bias	R ²	Nash-Sutcliffe	mean bias	R ²	Nash-Sutcliffe
old seNorge v.1.1	+200 mm	0.71	-0.54	0.100 kg/L	0.26	-1.70
new seNorge v.1.1.1	-5 mm	0.68	0.61	-0.001 kg/L	0.30 (0.38)*	0.30 (0.37)*

* values in parentheses apply for ρ when *SWE* > 100 mm.

In addition, comparison with snow depth (*SD*) measurements from MET-stations (totally ~400 000 measurements, see Saloranta 2012) show that the new version gave similar or better results compared to the old v.1.1 model. Especially the spring overestimation in *SD* is corrected in the new version and the number of “good match”-stations in the end of April is significantly increased. Namely:

- In evaluation (Saloranta 2012) of the old version (v.1.1) the average station-wise median bias was within -14 to +22 % from January through March. At the end of April, however, the median bias was +25 % in the 0-200 m a.s.l. bin, and as much as +108 % in the 400-600 m a.s.l. bin. The percentage of “good match”-stations was 72-83% before April, but decreases to 42 % at the end of April.
- The same evaluation made for the new version (v.1.1.1) shows that the average station-wise median bias is within -12 to +17 % all the way from January to the end of April. The percentage of “good match”-stations is 76-84% before April, and still 65 % at the end of April.

It is worth bearing in mind, however, that the MET-data (*SD*) is not perfectly well-suited for model evaluation and can give somewhat biased results in model evaluation. This is due to the fact that the bias in the gridded input data is likely less (but not zero) at the grid cells containing MET stations, than at the most other model grid cells, where the interpolation error is larger. In addition, biased simulations of *SWE* and ρ can potentially give a good match with *SD* for wrong reasons. In fact, this was the case in the old version (v.1.1), where significant overestimation errors in both *SWE* and ρ compensated each other, resulting in a more reasonable fit with *SD*. Due to these two aspects, the MET-data was not used in the parameter estimation (MCMC simulation).

2.2.1 Discussion

All in all, it is a rather difficult task to optimally adjust the over 6 000 000 000 seNorge model simulated values for each snow variable (*SWE*, *SD*, ρ) with help of a few hundreds or thousands observations. One has to operate in four dimensions (latitude, longitude, elevation, time), and make many subjective choices underway on, e.g., how to choose a representative set of observations for the whole Norway, how to handle zero-values and whether to minimize the absolute or the relative difference between model and observations (absolute difference was selected in our case).

The revisions made to the new snow maps seem to contribute to better overall snow map quality, as the large systematic biases have been mostly removed (better accuracy), and the physical process description of the model has improved. However, the map quality will still vary in both space and time, as in the previous version. Future research efforts should therefore focus more on studying the sources of variability in the model fit with observations (i.e. model precision). Namely, the adjustments made to the new snow model version have, somewhat disappointingly, not lead to very significant reductions in this variability (i.e. better model precision), although the model accuracy was significantly increased. It is uncertain whether this variability stems mainly from the input data, observations or the model. Further seNorge model development, comparison with other snow models, and use of other data sources in model evaluation may cast more light on whether a significantly better precision is achievable in snow mapping in Norway.

The guiding principle in the model revision has been “right results for the right reasons”. Thus, only those parameters that could be reasonably estimated on the basis of the *SWE* and ρ observations were included in the parameter estimation procedure (MCMC simulation). Although inclusion of other parameters, such as the maximum water content in the snow pack or new snow density, could have led to even better model fit, these parameters seemingly cannot feasibly be estimated on the basis of the *SWE* and ρ observation set sampled only twice in the snow season. Notice also that the revised parameter set (section 2.3) is optimized against the particular selected data set, and thus sampling a new, equally representative dataset, would certainly lead to slightly different optimal value set. This underlines the fact that there is not a single universally “best” parameter set, but that a certain uncertainty will always be connected to the optimized parameter values. This uncertainty is actually taken into account and estimated in the MCMC simulation, which estimates optimized *parameter distributions* instead of optimized single values. However, in this research note (and in the operational seNorge model application) a single set of optimal parameter values had to be selected from the joint distribution of estimated parameters.

The adjustments made into input snow precipitation along grid cell elevation are made on the basis of the whole history of snow maps back to 1957. Consequently, if the meteorological station network used in the interpolation of the input data (i.e. in producing the temperature and precipitation maps) is *significantly* changed, especially by introducing more stations at the higher elevations, then the input correction made in the snow model may need revision. The best future alternative would therefore probably be, that the biases with elevation in the precipitation maps, as indicated by this study and in Saloranta (2012), are corrected already in the making of the precipitation maps (by e.g. re-adjusting the precipitation lapse rates and/or catch correction factors), making eventually the rough overall input corrections in the snow model superfluous.

For more details on the model revisions, sensitivity analysis and MCMC simulation, see Saloranta (2014).

2.3 Revised seNorge snow model (v.1.1.1) parameter values

Parameters connected to the snow accumulation

- max. fraction (W_L/W_T) of liquid water (*PRO*): $PRO=0.11$
- correction factor f_s (*SKORR*) of snow precipitation with elevation (z)
 - if $z < 184$ m a.s.l. $f_s = 1$
 - if z is between 184 and 710 m a.s.l. $f_s = 1/(10^{[-0.073 + 3.96e-4*z]})$
 - if $z > 710$ m a.s.l. $f_s = 0.619$

Parameters connected to snow melt

- the daily melt algorithm parameters (b_0, c_0)
 - below treeline $b_0= 2.13$ mm/d/C° and $c_0= 6.3$ mm/d.
 - above treeline $b_0= 1.81$ mm/d/C° and $c_0= 10.9$ mm/d.

Parameters connected to the snow compaction and density

- the constant (ρ_{ns_min}) in the equation for density of new snow, i.e. density of new snow at 0 °F (= -18 °C) :
 - below treeline $\rho_{ns_min} = 0.050$ kg/L.
 - above treeline $\rho_{ns_min} = 0.100$ kg/L
- the parameter (C_6) of density effect on snow viscosity: $C_6 = 24.3$ L/kg

- the max compaction change (“*MaxChange*” in C-code) per time step is set to 0.5
- the max allowed density (“*MaxDensity*” in C-code) is set to 0.55 kg/L

Parameters connected to the new SCA-routine

- the *SWE* variability factor (f_{var}):
 - below treeline $f_{var} = 0.25$
 - above treeline $f_{var} = 0.50$

3 Daily snow melt rates in Norway: observations and modelling

The quantification and prediction of the snow melt rate is important among others in forecasting of floods (e.g. Midttømme et al. 2011) and the risk of slush flows and landslides. More accurate simulation of the snow melt rates will also enhance the quality of the snow maps for Norway, as simulated by the seNorge snow model.

In this section, snow melt rates are derived from the daily time series of snow water equivalent (*SWE*) from 31 snow pillow stations spread across Norway. These values are used to quantify the distribution of snow melt rates and to evaluate, calibrate and revise the degree-day based simple snow melt algorithm in the seNorge snow model. These revisions are implemented in the new version of this model (v.1.1.1).

3.1 Data and Methods

3.1.1 Data description

The time series of *SWE* from the 31 snow pillow stations were downloaded from the NVEs “HYDAG” database by the routine “seriestable”. Versions¹ 1 and 2 (if available) of the data were used in this analysis. In total 34 different time series were downloaded from 31 snow pillow stations (3 stations had both versions 1 and 2; the arctic station on Svalbard was omitted). The data spans years from 1967 to 2011 and the elevations from 35 to 1435 m a.s.l. The daily time series represent average *SWE* over a 24-hour period from midnight to midnight (local winter time, UTC+1).

The 125033 values in the raw *SWE* data, from 441 snow seasons, ranged from –999 to 1431 mm. All values < 50 mm were set to zero (54 % of all values), in order to avoid errors in the melt rate calculations in the late melting season when the snow pack is thin, patchy and disintegrating. The difference in *SWE* between two consecutive days ($\Delta SWE_t = SWE_t - SWE_{t-1}$) was then calculated, and the days where $SWE_t = 0$ were set to “NA”, in order to avoid partial melting values in the snow melt time series (i.e. melting down to bare ground). Figure 2 shows the spatiotemporal distribution of the snow pillow stations and *SWE* data.

The daily mean temperature and sum of precipitation, as well as the simulated *SWE*, were extracted from the seNorge data archives. The temperature and precipitation represent values interpolated from available meteorological observations to a grid with 1 x 1 km resolution (Tveito et al. 2002, 2005). Data from the grid cells corresponding to the snow pillow stations were used, unless the elevation difference between the snow pillow stations and the grid cell was more than 100 m, which was the case for two stations (Figure 2). Since the daily mean temperature and sum of precipitation for the current day are in the seNorge data calculated for the period from 06:00 UTC the day before to 06:00 UTC the current day, and the mean daily

¹ A new version of the time series usually means new instrumentation at the same site. Note that one station (Svarttjørnbekken) had up to 7 versions available in the period 2006-2010 (only versions 1 and 2 used here).

SWE is assumed to represent values around 15:00 UTC (middle of the assumed daily main melt period), a weighed average (5/8 of the current and 3/8 of the coming day) is used in order to better synchronize these variables with the daily melt rates (ΔSWE_t) derived from the snow pillow data.

For the snow melt study, a subset of the ΔSWE_t data was made, consisting only of negative values (i.e. melting). In addition, melt rates were only calculated from SWE values, which were recorded in the main melting season, from April to mid-July (daynumbers 91-196), and which were below 95 % of the SWE at last snow accumulation event. The latter criterion was applied in order to avoid small noise-like variations in recorded SWE at the very onset of melting (Heidi Stranden, pers. comm.), and to increase the chances that the snow pack is wet for the period when melt rates are calculated. Namely, in order to convert the decrease in SWE to melt rate, one has to assume that most of the melt water is drained out of the snow pack during the day. Finally, data from all the 441 snow seasons were visually investigated (by T. Skaugen and T. Saloranta), with focus on the melt season, and all snow seasons with dubious-looking data were removed from the dataset (109 of the 441 seasons were removed).

The melt rate is defined as $M = -\Delta SWE_t$ [mm/day] and the degree-day coefficient $C_M = M/T$ [mm/°C /day], where T is the daily air temperature [°C] extracted from the seNorge data archives. The melt rate data subset contains 5353 values after the first data screening described above (see Figure 3 for example of SWE data).

In the second screening, the melt rate data was binned according to the corresponding air temperature T (1 °C bins). Melt values were discarded from those bins which contained less than 40 values of M , and where more than 5 % of the M values were below the assumed snow pillow detection limit for M , set here to 3 mm/day by the author's expert judgement. After this screening, only the M data where $M \geq 3$ mm/day and where the corresponding air temperature is in the range 2-12 °C remained. Moreover, 66 potential outlier values of M (i.e. values outside the fitted 1 and 99 % quantile regression lines) were removed.

Finally, after all data screening steps, 3356 values of M remain for the analysis, and the 1, 50 and 99 % percentiles for the distribution of M in this final data set are 4, 15 and 45 mm/d, respectively (maximum value is 65 mm/d).

As in the seNorge model, the data set is divided into two station classes, namely "forest" (including both light and denser forest) and "treeless". The station classification was done manually by Heidi Stranden, NVE (one station remains to be classified). The station classification does not necessarily match the classification used for the whole 1x1 km grid cells in the seNorge model.

All the data analysis was made in the statistical software "R" (www.r-project.org) by the script "snowpillow.data.arrange.v2.R".

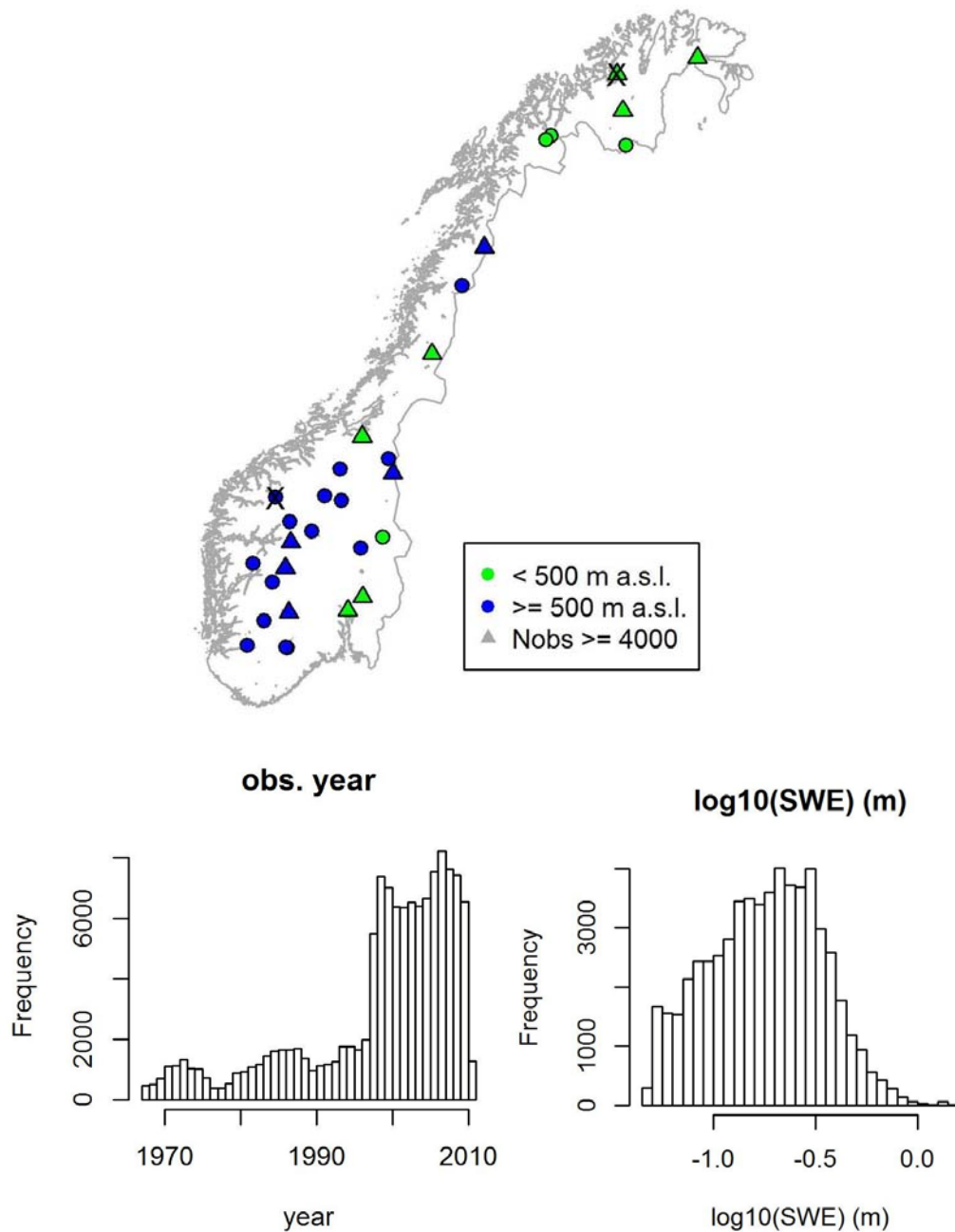


Figure 2. Map showing the location, as well as classification of station elevation and time series length of the 31 snow pillow stations. Note that the southernmost point masks the other station situated very close, but at a lower 330 m a.s.l. elevation. The two crosses denote stations for which the temperature data from the seNorge-grid was not used, as the difference between station and grid cell elevation was > 100 m. The histograms show the distributions of the observation year and \log_{10} -transformed SWE (units here in meters; values of SWE < 50 mm are set to zero) in the snow pillow data.

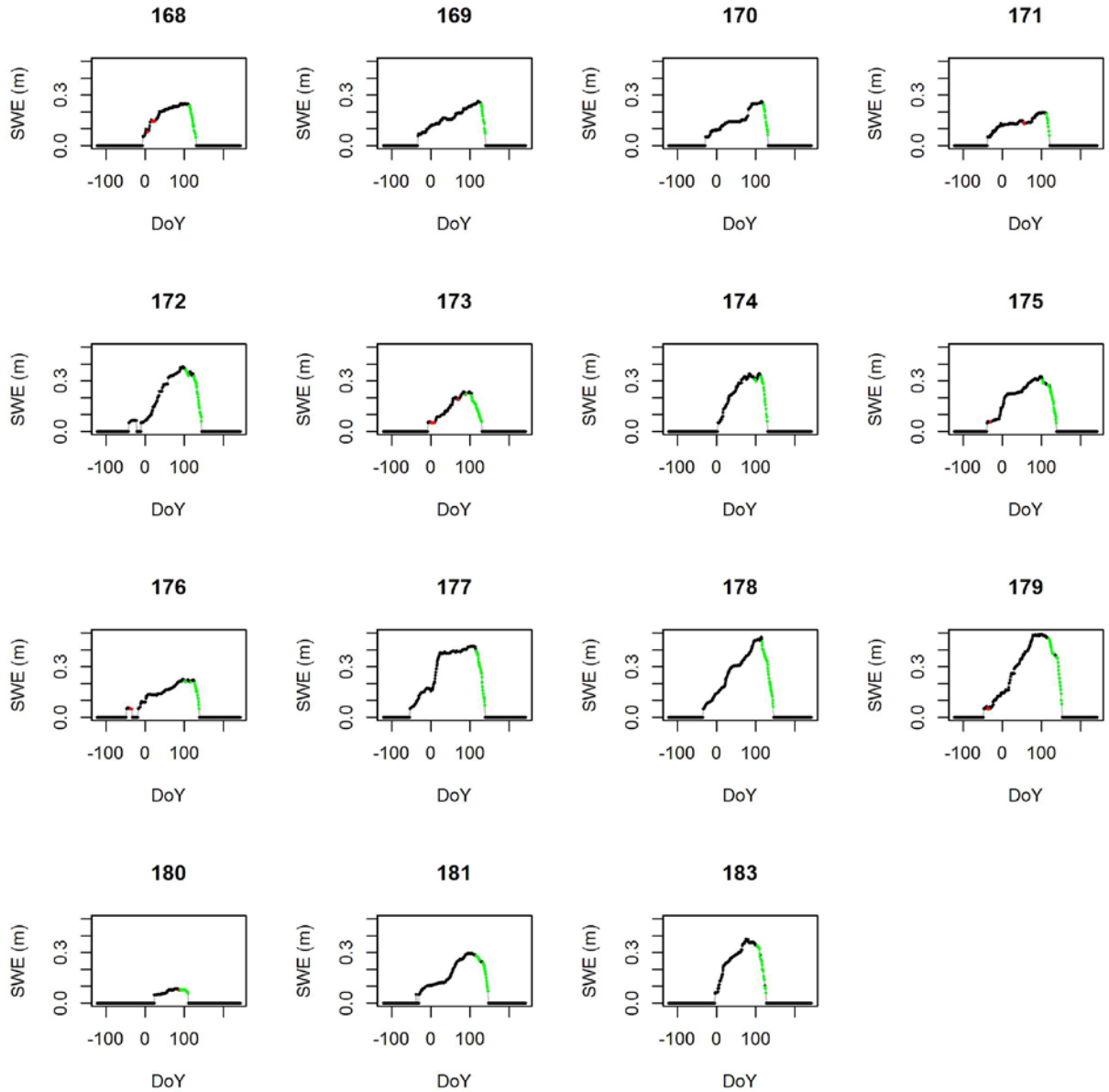


Figure 3. Example of the seasonal evolution of SWE in NVE snow pillow data from 15 snow seasons (i.e. hydrological years starting at September 1) after first stage of data screening (see text for details). Red and green dots denote the days which fulfill criteria for the snow melt data subset. The green values are the ones finally selected for this subset (i.e. which are inside the time-window from April to mid July). “DoY” on the x-axis denotes the day of the year (i.e. N_d ; 1 = January 1, etc.).

3.1.2 The previous (v.1.1) seNorge snow melt algorithm

In the previous seNorge snow model (v.1.1) the degree-day approach was used, and snow melt rate M was assumed to be proportional to T , whenever T is above the melt threshold temperature ($T_M = 0$ °C), i.e.

$$M = b_0 T \quad (1a)$$

where the coefficient b_0 is equal to the degree-day coefficient C_M . Furthermore, in the previous seNorge model, C_M was assumed to be a function of the day of the year, latitude and vegetation type (below/above treeline), attempting to approximate roughly the variation in the short-wave radiation flux. The variation of C_M along the time of the snow season was approximated by a sinus-wave between C_{Mmin} and C_{Mmax} reaching its maximum at the summer solstice (around 21 June):

$$C_M = C_{Mmin} + (C_{Mmax} - C_{Mmin}) \cdot D \quad (1b)$$

where D varies between 0 and 1 in a sinus-like form between the winter and summer solstices

$$D = 0.5 \cdot (\sin(2\pi((N_d - 81.5)/366)) + 1) \quad (1c)$$

and where N_d is the number of the current day in the current year.

3.2 Results

3.2.1 The new revised seNorge (v.1.1.1) snow melt algorithm

Figure 4 shows M plotted against T , and the linear regression lines fitted to the data (both “ordinary” and quantile regression), as well as to the means calculated for each of the 1 °C bins. The regression lines fit well with the corresponding bin means and percentiles (Figure 4), indicating that the simple linear model is adequate in describing the melt rates as a function of T . Figure 4 shows that the regression lines do not go through the origin, but that there is some melting still on average, even though $T = 0$ °C. This is not in accordance with the simple degree-day melt equation (Eq. 1), which can be improved with an additional temperature-independent term (a_0).

$$M = a_0 + b_0 T \quad (2)$$

The additional term (a_0) can be thought to represent e.g. the short-wave radiation flux, which can cause melting even if T is somewhat below zero, while the second term ($b_0 T$) can be thought to represent the turbulent (sensible) heat flux, dependent on the difference between the snow surface (= 0 °C at melting) and air temperature. Observed melting at $T = 0$ °C could also be partly due to systematic bias in T , and/or variation of T during a day, not captured by the daily mean T . However, no significant systematic bias in T has been detected, and the linear shape of the curves in Figure 4 do not indicate any significant error due to diurnal variation of T .

Values for a_0 and b_0 were estimated using ordinary regression analysis. The fit was now better than when using Eq. 1, but residuals (not shown) from this analysis had still a slight trend along the snow season.

If the term a_0 in Eq. 2 is interpreted to be due to the shortwave radiation heat flux, then it follows that this term should also change with time of the year and latitude (according to standard astronomical formula). This variation was already attempted to be taken into account in the previous seNorge snow melt model (section 3.1.2), but was actually affecting the degree-day coefficient (b_0 ; see Eq. 1b) instead of the offset term (a_0), which was not included at all in this

model version. This may be somewhat too simplified way of modelling, where the effects of short-wave radiation and turbulent (sensible) heat flux are both “lumped” into the same degree-day coefficient $b_0 (=C_M)$. However, in reality the shortwave flux is not causally very dependent on T , but mostly dependent on the day of the year, latitude, and atmospheric transmissivity (clouds, etc.). Therefore, these two terms are separated, as in Equation 2.

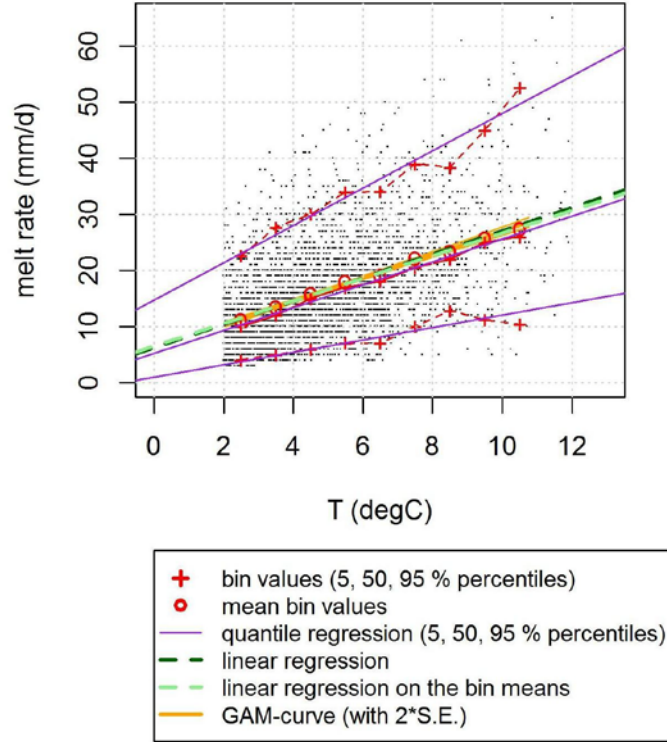


Figure 4. The melt rate vs. temperature in the data after all quality screening steps (3356 melt rate observations). The different curves for bin statistics, regressions and GAM-fit are explained in the legend.

On the basis of the more physically realistic snow melt process described above, as well as of the results from the residual analysis, Eq. 2 is modified further to include a time-varying term $c_0 S^*$, where c_0 is a constant and S^* is the potential extraterrestrial solar radiation on a horizontal plane, normalized by the maximum value at the latitude 60°N (see Table 2 for value examples).

$$M = a_0 + b_0 T + c_0 S^* \quad (3)$$

The potential extraterrestrial solar radiation on a horizontal plane S [$\text{MJ}/\text{m}^2/\text{day}$] is a function of the day of year (N_d) and the latitude (ϕ), and can be readily estimated from well established astronomical formula (see e.g. Walter et al. 2005). Thus, $S^*(\phi, N_d) = S(\phi, N_d) / (S(\phi=60^\circ\text{N}, N_d=172))$. The use of S^* (instead of S) simplifies the interpretation of c_0 somewhat as it has the meaning of maximum added melting due to the time-varying term at the latitude 60°N (and roughly in Norway in general) at the summer solstice. The seasonal dependency introduced by the new variable S^* did improve model fit slightly, by diminishing the dependency of model residuals on the day of the year and latitude.

Table 2. Examples of seasonal variation of S^* values at 60 and 70 °N.

	31 January	28 February	31 March	31 April	31 May
<i>at 60 °N</i>	0.12	0.28	0.53	0.78	0.96
<i>at 70 °N</i>	0.01	0.13	0.40	0.71	0.96

To further simplify the model, the constant offset term a_0 was ignored assuming that $M=0$ at polar night conditions (no daily sunshine) and at $T=0^\circ$ C. This simplification did not have any significant effect on the R^2 values or model residual distribution.

Thus, the final revised melt model version is

$$M = b_0 T + c_0 S^* \quad (4)$$

Values for b_0 and c_0 were estimated using multiple regression analysis (note that the estimation of c_0 is based on values of M from the spring and summer only).

For the “forest” class the optimized $b_0 = 2.13$ mm/°C /day and $c_0 = 6.3$ mm/-/day, respectively. The observed total sum of melt was estimated exactly by the optimized model, while the previous seNorge model (v.1.1) underestimated the observed total sum of melt by 7 % for the “forest” class.

For the “treeless” class the optimized $b_0 = 1.81$ mm/°C /day and $c_0 = 10.9$ mm/-/day, respectively. The observed total sum of melt was estimated exactly by the optimized model, while the previous seNorge model (v.1.1) underestimated the observed total sum of melt by 13 % for the “treeless” class.

The most significant difference between the estimated parameter values of “forest” and “treeless” classes is in the c_0 , which is much lower for the “forest” class. This lower value can easily be explained by the shading effect of the canopy for the shortwave radiation dependent part, approximated by $c_0 S^*$ term in Eq. 4. The degree-day coefficients in the previous seNorge snow model were similarly lower for the “forest” than for the “treeless” grid cells.

Table 3 shows the NS -values (Nash-Sutcliffe measure) for M , indicating the performance of the different models (the larger the NS the better the model fit). The NS -values show that the revised model gives better fit than the current seNorge model, especially for the “treeless class”. The model fit was only marginally improved from that of Eq. 2 to Eq.4. However, as already pointed out above, the physically more realistic melt processes is the main reason why Eq. 4 is preferred over Eq. 2.

The absolute difference between modelled and observed M were in 95 % of the cases within -17 to $+11$ mm/day (-19 to $+12$ mm/day) for the “forest” (“treeless”) class.

Figure 5 shows the observed melt rates vs. temperature for the two station classes (“forest/treeless”), together with bin means and some fitted univariate regression lines, as well as the distribution of melt rate model residuals (from Eq. 4) and their dependence on T and N_d . Note that the dependencies in the melt rate model in Eq. 4 (multivariate regression model) cannot be easily illustrated in a single figure, due to its dependency on three covariates, i.e. $M = f(T, \phi, N_d)$.

Table 3. The *NS*-values (Nash-Sutcliffe measure) indicating the goodness of the fit of *M* simulations from the three different snow melt models.

Model	<i>NS</i> for "forest" class	<i>NS</i> for "treeless" class
<i>seNorge</i> (v.1.1)	0.31	0.03
Eq. 2	0.34	0.18
Eq. 4	0.35	0.20

(a) "forest" class

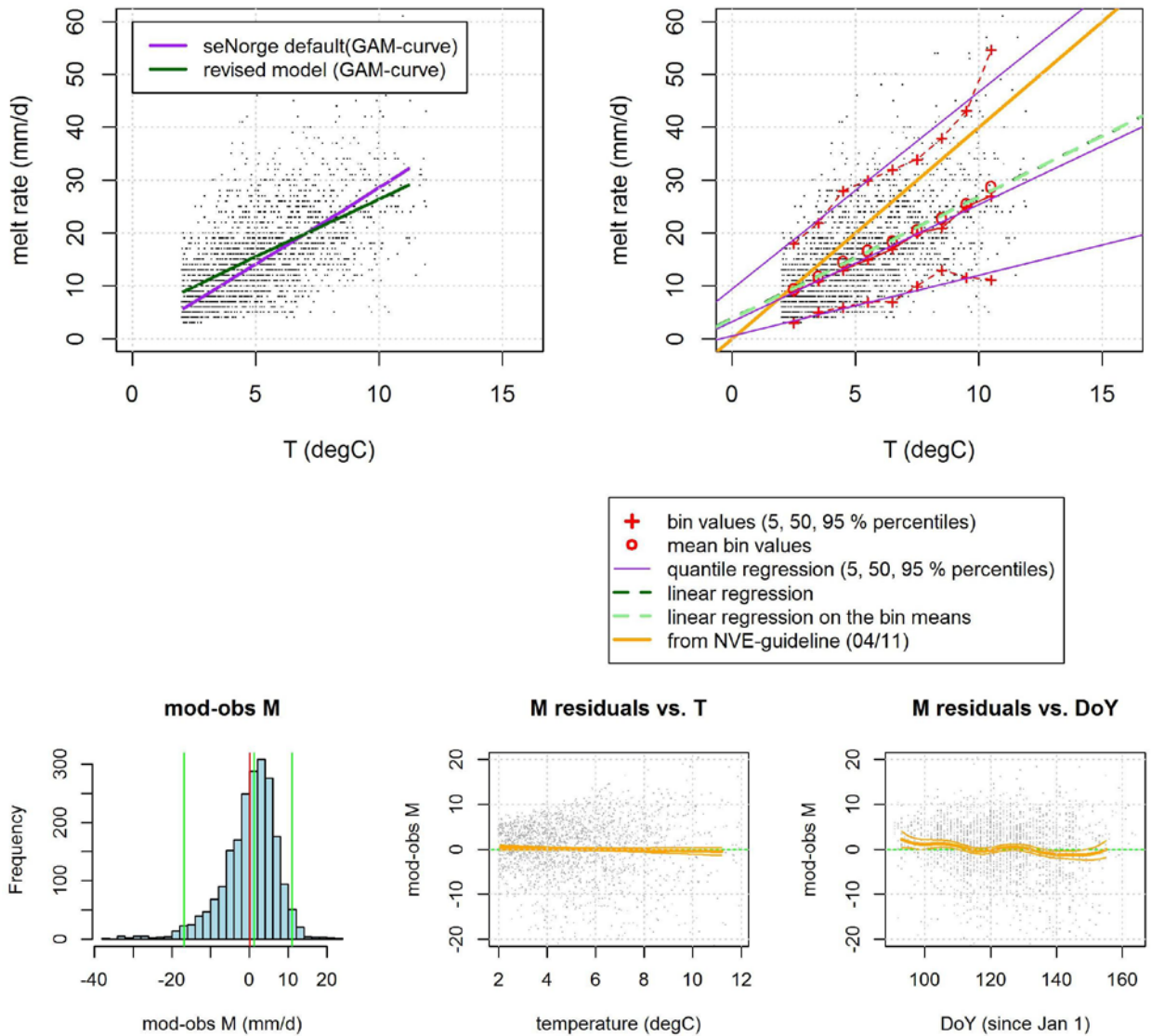


Figure 5. (continued on next page).

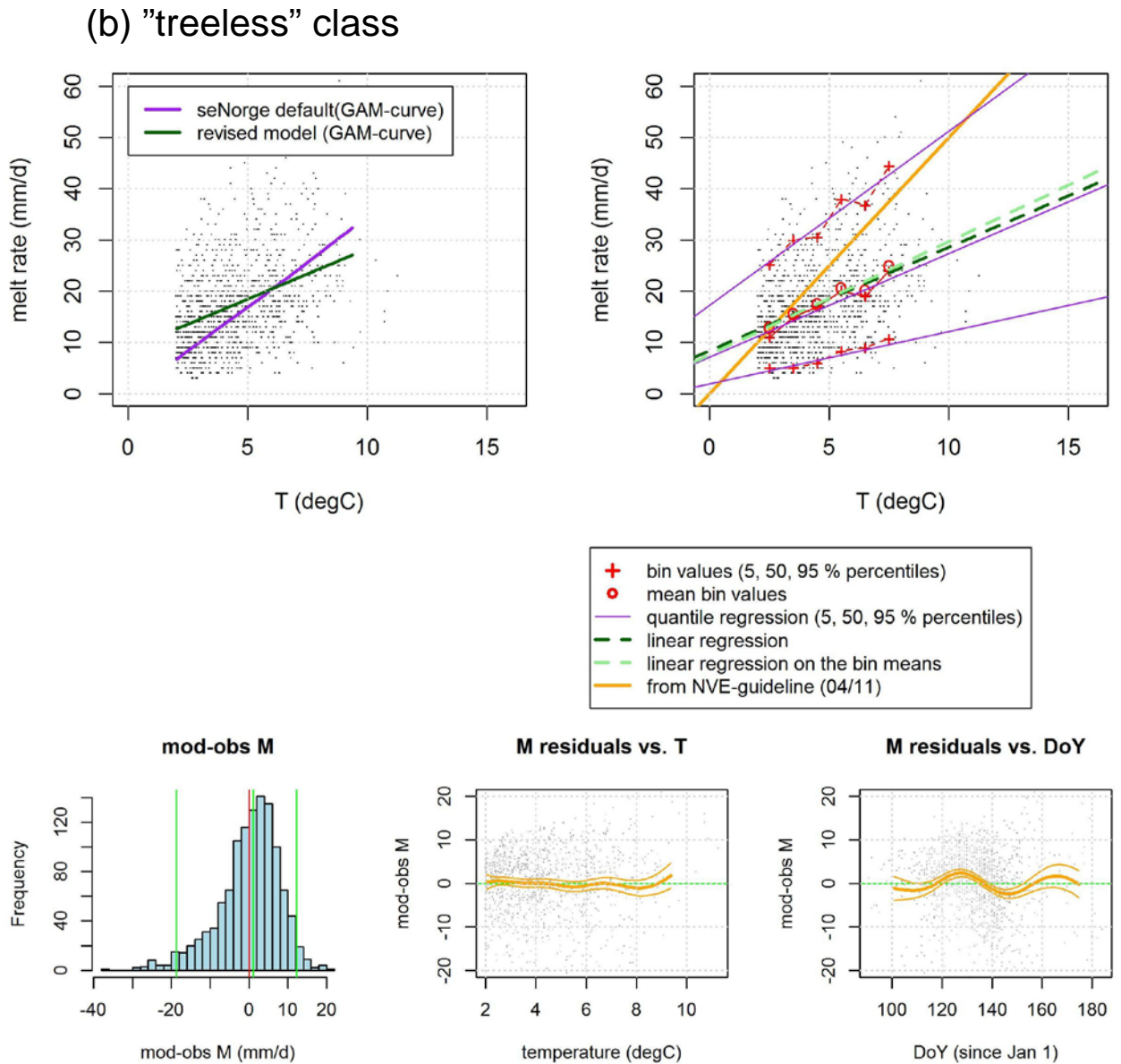


Figure 5. The melt rate statistics for the (a) “forest” class (light and denser forest) and (b) “treeless” class. **Upper left panels:** Observed melt rate vs. temperature (points) and GAM-curves fitted to the corresponding simulated melt rates (seNorge (v.1.1) vs. Eq. 4; see legend). **Upper right panels:** Melt rate vs. temperature, as in Fig. 4, but now plotted separately for the two data subsets (“forest” and “treeless” class). Note that the orange lines now denote the melt rates based on the degree-day model ($C_M = 4$ and $5 \text{ mm}^\circ\text{C}/\text{day}$ in (a) and (b), respectively) in the NVE-guidelines for flood estimation (Midttømme et al. 2011). **Lower panels:** Distribution of melt rate model residuals (Eq. 4) and their dependence on temperature and day of the year (“DoY” = N_d used in the text). The green and red lines in the histogram denote the 2.5, 50, 97.5 % percentiles and the mean value, respectively. The orange lines denote fitted GAM-curves, with uncertainty bounds (± 2 times the standard error).

3.2.2 “Extreme value” models

In order to provide an alternative model for the more “extreme” melt rates, a 95 % quantile regression (QR) model was also fitted to the data. This means that only 5 % of the values of M are estimated to be above this regression line. In this QR-model the optimized b_0 and c_0 become 3.61 (3.54) mm/°C /day and 12.2 (19.0) mm/-/day, respectively, for the “forest” (“treeless”) class. These values can be compared to the melt rates calculated on the basis of the degree-day model ($C_M = 4$ and 5 mm/°C /day for light forest and treeless terrain, respectively) in the NVE-guidelines for flood estimation (Midttømme et al. 2011). These guidelines are meant to be used e.g. in helping to design safe dimensioning of hydropower dam constructions.

For example, at $T = 10$ °C, the NVE-guidelines give melt rates of 40 and 50 mm/day for light forest and treeless terrain, respectively, while similar values from the QR-model at summer solstice (June 21) are 48 and 54 mm/day, respectively. The QR-model gives thus slightly higher values than the NVE-guidelines in midsummer at $T = 10$ °C. At even higher temperatures (> 10 °C) the difference between the two approaches diminishes further (and even changes sign), as indicated in Figure 5.

3.3 Summary

The over 125 000 daily observations of SWE from over 30 snow pillows spread across Norway were reduced in data screening to 3356 quality-checked melt rate (M) values. These were combined with air temperature taken from gridded meteorological observations (www.seNorge.no) and other covariates, such as day of year, latitude etc., in order to analyse the melt rate dependencies on these covariates, and to revise the melt rate algorithm used in the previous seNorge (v.1.1) snow model.

- The 1, 50 and 99 % percentiles for the distribution of M in the final data set were 4, 15 and 45 mm/d, respectively (maximum value was 65 mm/d).
- The regression lines fitted to the data correspond well with the calculated 1 °C bin means and percentiles (Figure 4), indicating that the simple linear model approach is adequately describing the melt rates as a function of T .
- However, the data indicates that the basic degree-day model used in the previous seNorge (v.1.1) snow model (Eq. 1) should be revised with an extra term, as the regression line does not go through the origin (i.e. through $T=0, M=0$; Figure 3).
- The revised melt rate model (v.1.1.1; Eq. 4) provides a better fit to the melt rate data, and a more physically realistic melting, than the previous seNorge (v.1.1) algorithm. On average, the revised model simulates more melting than the seNorge algorithm at lower temperatures, and less melting at higher temperatures (see Figure 5).
- The revised melt rate model (Eq. 4), with temperature data from seNorge, gives an unbiased estimate to the observed melt rates. In terms of 95 % confidence limits of the daily predictions of M , the model fit ranges from an underestimation of M by roughly 20 mm/day to overestimation by roughly 10 mm/day. This variability is due to uncertainties i) in the melt rate model (Eq. 4), ii) in the input data (T values from seNorge), and iii) in the observations of M .

- The “extreme values”, estimated by the QR-model, are somewhat higher than those based on the NVE-guidelines (Midttømme et al. 2011) at $T = 10\text{ °C}$, but still in the same order of magnitude. At even higher temperatures ($> 10\text{ °C}$) the difference between these two approaches diminishes further (and even changes sign), as indicated in Figure 5.

In the future studies, the analysis could be refined e.g. by investigating the effect of precipitation as an additional covariate, and by applying T data with higher temporal resolution (3 h). Also discharge measurements during an extreme snow melt situation in spring 2010 could be analysed and compared e.g. to the “extreme values” from the QR-model (section 3.2.2).

4 New algorithm for subgrid snow distribution and fraction of snow-covered area in the seNorge snow model.

4.1 Introduction

Snow depth (and snow water equivalent, *SWE*) shows a strong spatial variability (see e.g. the review by Clark et al. 2011). For example, in mountainous areas the interplay of topography and wind redistribution of snow can cause snow depths to vary from zero (bare ground) to a few meters on a short distance (tens of meters).

In the previous seNorge snow model (v.1.1), no variability of snow depth (or *SWE*) was assumed within the model 1x1 km grid cells. In other words, snow was assumed to have even thickness everywhere within a grid cell. In order to improve this part of the model, a new algorithm is developed for the revised model version v.1.1.1, inspired by the snow distribution algorithm in the VIC model (Cherkauer et al. 2003). The new algorithm describes 1) the subgrid variability in *SWE* and 2) the fraction of snow-covered area (*SCA*) within the seNorge model grid cells. The algorithm assumes that snow is distributed as the uniform distribution within the grid cells, i.e. that all *SWE* values between a defined minimum and maximum value are equally likely within a grid cell (Figure 6). In addition, if $SCA < 1$, an even layer of new snow can form on top of the uniformly distributed “old” snow pack (SCA is set to 1). If this new snow layer is completely melted again, the *SCA* value of the “old” snow pack ($SCA < 1$) beneath the new snow layer is used again.

The main effect of the subgrid snow distribution is to reduce the grid cell average melting rates in the late melt season, when part of the grid cell is bare ground (i.e. $SCA < 1$) (see Figure 7).

The “box-shaped” uniform distribution is one of the simplest probability distributions, but has several advantages in the snow distribution algorithm, as it is i) simple to integrate, ii) preserves its “form” even when truncated, and iii) is symmetric around the mean value.

In the following section the snow distribution algorithm is described in more details. Note that it is the ice fraction (in water equivalents, *SWE_i*) of the snow pack which is used in the following calculations. Moreover, no spatial dependence of the melting rates is assumed, and the same order of processes as in the seNorge density algorithm is assumed (melting of the old snow pack \Rightarrow new snow fall \Rightarrow melting of the new snow fall).

4.2 The algorithm description

The mean ice water equivalent (*SWE_i*) [mm] of the snow pack in a grid cell is divided into two parts:

$$SWEi = SWEi_{pack} + SWEi_{buff} \quad (5)$$

where the $SWEi_{pack}$ and $SWEi_{buff}$ represent the mean depths [mm] (in a grid cell) of the uniformly distributed snow pack and the layer of new snow ("new snow buffer"), respectively (see Figure 6).

The variability range around $SWEi_{pack}$ is assumed to be proportional by a factor f_{var} to the highest $SWEi_{pack}$ reached so far in the snow season ($SWEi_{HI}$), so that the minimum and maximum values of the uniformly distributed snow pack ($SWEi_{min}$, $SWEi_{max}$) are equal to $SWEi_{pack} \pm f_{var} \cdot SWEi_{HI}$. This range is hereinafter denoted by $R (= f_{var} \cdot SWEi_{HI})$.

The algorithm utilises an "untruncated" version of the uniformly distributed snow pack (see Figure 6; variables here denoted by asterisk "*"), where melting can continue in a hypothetical way below bare ground, and where negative $SWEi_{min}^*$ or $SWEi_{pack}^*$ can occur ($SWEi_{max}^* = SWEi_{max}$, however). Thus,

$$SWEi_{pack}^* = SWEi_{pack} \quad , \text{ if } SCA_{pack} = 1 \quad (6a)$$

$$SWEi_{pack}^* = 2\sqrt{SWEi_{pack} \cdot R} - R \quad , \text{ if } SCA_{pack} < 1 \quad (6b)$$

where SCA_{pack} is the SCA -value of the uniformly distributed snow pack (i.e. excluding the layer of new snow). It is easily seen that $SCA_{pack} < 1$, if $SWEi_{pack} < R$. The Eq. 6b results from solving the roots of a second degree polynomial (see section 4.2.1).

The exact value of the SCA_{pack} (if any snow is left) is calculated as:

$$SCA_{pack} = \frac{SWEi_{pack}^*}{2R} + 0.5 \quad , \text{ where } SCA_{pack} \text{ is truncated to interval } [0,1]. \quad (7)$$

The first option ("if-structure") in the algorithm handles the case, where the new snow layer *is not* completely melted during the time step. In this case the melting is subtracted and new snow fall and refreezing are added to the new snow layer $SWEi_{buff}$. All the other variables are kept unchanged at this stage. SCA is naturally equal to 1, as the layer of new snow always is assumed to cover the whole grid cell (except for very thin new snow layer, see below).

The second option ("else-structure") in the algorithm handles the opposite cases, where either the new snow layer *is* completely melted during the time step, or no new snow layer exists at the start of the current time step. In these cases the following updates are made to the snow variables:

Alternative 1: If $SCA < 1$ either at the start or the end (due to melting) of the current time step:

- The updated $SWEi_{pack}^*$ is calculated by subtracting melting from the $SWEi (= SWEi_{pack} + SWEi_{buff})$ of the previous time step, or just adding refreezing to the $SWEi_{pack}^*$ of the previous time step. The $SWEi_{max}$ is updated in a similar way.
- The updated SCA_{pack} is calculated as in Eq.7.
- $SWEi_{pack}$ is updated, based on the updated SCA_{pack} :

- if $SCA_{pack} = 0$ (bare ground before or after melting) $SWEi_{pack}$ is equal to the new snow fall (subtracting any remaining melt that can be left if the “old” snow pack was completely melted). $SWEi_{buff}$ remains zero.
- if SCA_{pack} is between 0 and 1 (partly snow covered grid cell) $SWEi_{pack} = 0.5 \cdot SWEi_{max} \cdot SCA_{pack}$. New snow fall (if any) is added to $SWEi_{buff}$ (which went to/was zero at the start of the second option stage).

A special case can occur, if the SCA_{pack} is slightly below 1 and refreezing has “lifted” the snow column back to a state where $SCA_{pack} = 1$. In this case $SWEi_{pack}$ is equal to the new snow fall added to the updated $SWEi_{pack}^*$. $SWEi_{buff}$ remains zero.

Alternative 2: If SCA is still equal to 1 after the melting in the current time step:

- The updated $SWEi_{pack}$ is calculated by subtracting melting (or adding refreezing) and adding new snow fall to the old $SWEi_{pack}$. $SWEi_{buff}$ remains zero.

After these two **Alternatives**, the algorithm checks whether the new snow layer (“buffer”) is full and should be redistributed and integrated to $SWEi_{pack}$. The maximum size of this buffer is set to $SWEi_{max}/(1+f_{var}) - SWE_{pack}$, and if $SWEi_{buff}$ exceeds this limit, $SWEi_{buff}$ is added to $SWEi_{pack}$ and reset (i.e. $SWEi_{buff}$ is set to zero). The value of $SWEi_{HI}$ is set equal to $SWEi_{pack}$.

After this, $SWEi_{HI}$ is updated if $SWEi_{pack} > SWEi_{HI}$. The $SWEi_{HI}$ is reset whenever the snow pack completely melts, or the new snow layer is integrated to $SWEi_{pack}$ (see above).

Finally, updated value of SCA for the grid cell is derived so that:

- if the new snow layer ($SWEi_{buff}$) exceed a threshold limit (currently set to 1 mm), then $SCA = 1$;
- if the snow cover is very thin, i.e. $SWEi$ is below a threshold limit (currently set to 1 mm), then $SCA = 0$;
- else $SCA = SCA_{pack}$.

The melt (or refreezing) reduction factor f_M (due to $SCA < 1$) is calculated, based on the ratio of change in $SWEi$ to the originally estimated melting (or refreezing). This factor is given as output from the algorithm and can be used to adjust the melt (or refreezing) rates in the snow model due to the effect of a partially snow-covered grid cell.

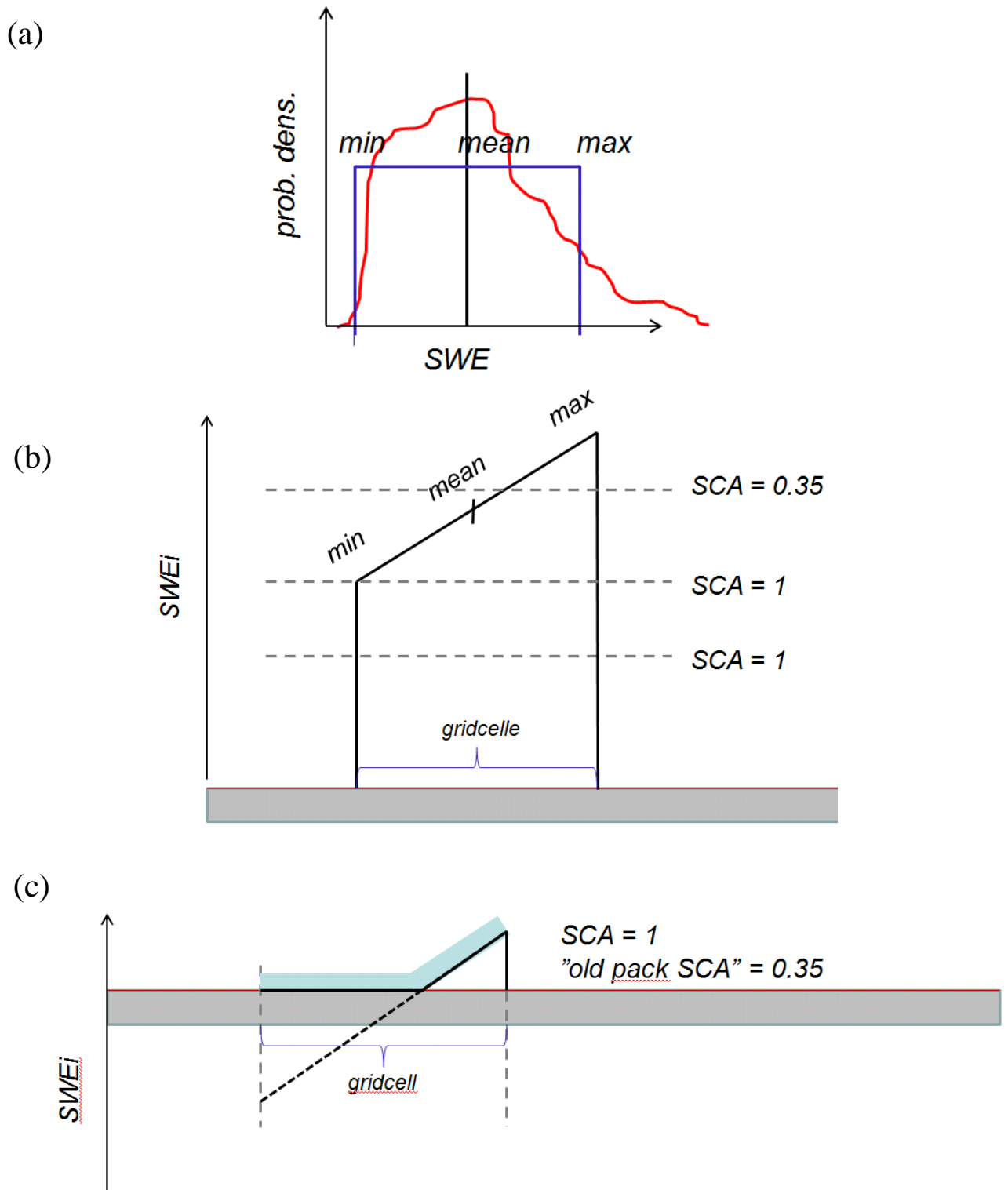


Figure 6. Schematic figures showing (a) “real” (red line), uniform (blue line) and no distribution of SWE (black line). (b) The uniformly distributed snow pack covering the whole grid cell. The dashed lines denote different “ground levels”, with corresponding SCA values shown. (c) The partly melted uniformly distributed “old” snow pack (solid black line; the fraction of snow covered area of the “old” pack is 0.35) with a layer of new snow on top (light blue). The black dashed line denotes the untruncated “imaginary” snow pack used in the calculations.

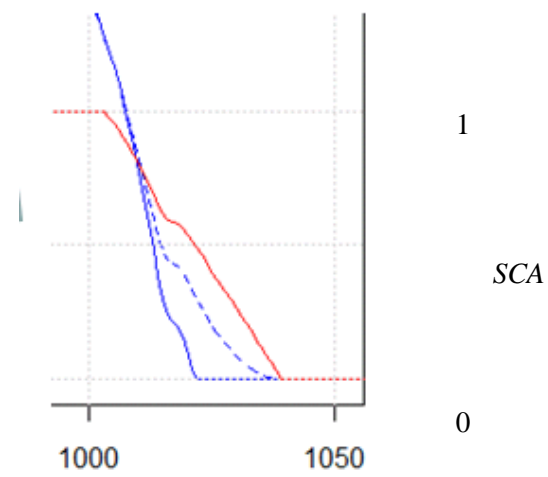


Figure 7. An example showing the snow melt evolution with (dashed blue line) and without (solid blue line) the snow distribution algorithm. The red line denotes the simulated snow-covered area (SCA).

4.2.1 Appendix: Details behind Equation 6b

If $SCA_{pack} < 1$, then combining SCA_{pack} from Eq. 7 with the fact that $SWEi_{pack} = 0.5 \cdot SWEi_{max} \cdot SCA_{pack}$ (when $SCA_{pack} < 1$) we get:

$$SWEi_{pack} = 0.5 \cdot (SWEi_{pack}^* + R) \cdot \left(\frac{SWEi_{pack}^*}{2R} + 0.5 \right) \quad (8)$$

By multiplying out the individual terms we get:

$$SWEi_{pack} = 0.25 \cdot \left(\frac{(SWEi_{pack}^*)^2}{R} + 2 \cdot SWEi_{pack}^* + R \right) \quad (9)$$

which is of the second degree polynomial form $ax^2 + bx + c = 0$, where $x = SWEi_{pack}^*$, and with coefficients $a = 1/R$, $b = 2$ and $c = R - 4 \cdot SWEi_{pack}$. The well-known formula for the roots of a second-degree polynomial is:

$$x = \frac{-b \pm \sqrt{b^2 - 4ac}}{2a} \quad (10)$$

This gives:

$$SWEi_{pack}^* = \frac{-2 \pm \sqrt{4 - 4 + 16 \left(\frac{SWEi_{pack}}{R} \right)}}{\frac{2}{R}} = R \cdot \left(-1 \pm 2 \sqrt{\frac{SWEi_{pack}}{R}} \right) \quad (11)$$

Finally, selecting the right one of the two roots, gives Eq. 6b.

$$SWEi_{pack}^* = 2 \sqrt{SWEi_{pack} \cdot R} - R \quad (12)$$

5 Conclusions

This report has summarized the revisions made to the new seNorge snow model (v.1.1.1). The evaluation of the new revised snow model (v.1.1.1; section 2) showed that the significant biases detected in the previous model version are removed, and the Nash-Sutcliffe model performance indicator has increased from the negative values of -0.54 and -1.70 for snow water equivalent and density, respectively, to the clearly positive values of 0.61 and 0.30. Comparison with snow depth data from meteorological stations show, among others, that the percentage of “good match” station in the spring (end of April) has increased from 42 % (v.1.1) to 65 % (v.1.1.1).

The revised melt rate model (section 3) is able to provide a better fit to the daily snow melt rate data from the NVEs snow pillows, and a more physically realistic melting, than the previous seNorge (v.1.1) algorithm. On average, the revised model simulates more melting than the seNorge algorithm at lower temperatures, and less melting at higher temperatures.

The new module for the snow distribution and fraction of snow-covered area (section 4) has contributed to extending the previous seNorge model from being a “point” model, where the snow within a grid cell was a homogeneous flat “blanket”, to the more realistic case where the depth of the snow cover can vary significantly within the grid cell. This allows also the grid cells to be partly snow-covered, which gives more realistic late spring snow melt evolution, where average melt rates are reduced and the snow (melt) season lengthened, until all the piles of snow in the grid cell are melted and only bare ground is left.

The operational version of this model was constructed by Jess Andersen at the NVEs section for Hydroinformatics, and has since autumn 2013 been producing a new set of more accurate snow maps, extending all the way from 1957 to the present (and even 9 days in the future).

Acknowledgements

Many thanks for Heidi Stranden for the snow pillow station vegetation type classification, and for Thomas Skaugen for his help and expert opinion in snow pillow data quality checking.

References

- Cherkauer, K. A., Bowling, L. C. and Lettenmair, D. P. 2003: Variable infiltration capacity cold land process model updates. *Global and Planetary Change* 38, 151-159.
- Clark, M. P., Hendrikx, J., Slater, A. G., Kavetski, D., Anderson, B., Cullen, N. J., Kerr, T., Hreinsson, E. Ö. and Woods, R. A. 2011: Representing spatial variability of snow water equivalent in hydrologic and land-surface models: A review. *Water Resour. Res.* 47, W07539.
- Dyrørdal, A. V. 2010: An evaluation of Norwegian snow maps: simulation results versus observations. *Hydrol. Res.* 41, 27-37.

- Engeset, R., Tveito, O. E., Alfnes, E., Mengistu, Z., Udnæs, H-C., Isaksen, K. and Førland, E. J. 2004a: Snow map system for Norway. *XXIII Nordic Hydrological Conference, 8-12 Aug. 2004, Tallinn, Estonia. NHP report 48(1)*, 112-121.
http://senorge.no/senorgeAux/NHC2004Tallinn_SnowMapSystem_Paper.pdf
- Engeset, R., Tveito, O. E., Udnæs, H-C., Alfnes, E., Mengistu, Z., Isaksen, K. and Førland, E. J. 2004b: Snow map validation for Norway. *XXIII Nordic Hydrological Conference, 8-12 Aug. 2004, Tallinn, Estonia. NHP report 48(1)*, 122-131.
http://senorge.no/senorgeAux/NHC2004Tallinn_SnowMapValidation_Paper.pdf
- Midttømme, G. H., Pettersson, L. E., Holmqvist, E., Nøtsund, Ø., Hisdal, H. and Sivertsgård, R. 2011: Retningslinjer for flomberegninger. NVE-retningslinjer 04/2011, Norwegian water resources and energy directorate (NVE), Oslo, Norway. 66 pp. (in Norwegian).
- Saloranta, T. M. 2012: Simulating snow maps for Norway: description and statistical evaluation of the seNorge snow model. *The Cryosphere* 6, 1323-1337.
- Saloranta, T. M. 2014: New MCMC-optimized version of the seNorge snow model and the snow maps for Norway. Manuscript in prep.
- Stranden, H. B. 2010: Evaluering av seNorge: data versjon 1.1. *Dokument nr 4/2010 Norges vassdrags- og energidirektorat (NVE)*, Oslo, Norway, (in Norwegian). 36 pp., 2010.
<http://www.nve.no/Global/Publikasjoner/Publikasjoner%202010/Dokument%202010/dokument4-10.pdf>
- Tveito, O.E., Udnæs, H.-C., Mengistu, Z., Engeset, R., and Førland, E.J. 2002: New snow maps for Norway. *Proceedings XXII Nordic Hydrological Conference 2002, 4-7 August 2002, Røros, Norway*, 527-532.
http://senorge.no/senorgeAux/NHC2002Roros_NewSnowMap_Paper.pdf
- Tveito, O. E., Bjørndal, I., Skjelvåg, A. O. and Aune, B. 2005: A GIS-based agro-ecological decision system based on gridded climatology. *Meteorol. Appl.* 12, 57-68.
- Walter, M. T., Brooks, E. S., McCool, D. K., King, L. G., Molnau, M. and Boll, J. 2005: Process-based snowmelt modeling: does it require input data than temperature-index modeling? *J. Hydrol.* 300, 65–75.

Denne serien utgis av Norges vassdrags- og energidirektorat (NVE)

Utgitt i Rapportserien i 2014

- Nr. 1 Energibruk i forretningsbygg
- Nr. 2 Det høyspente distribusjonsnettet. Innsamling av geografiske og tekniske komponentdata
- Nr. 3 Naturfareprosjektet Dp. 5 Flom og vann på avveie. Dimensjonerende korttidsnedbør for Telemark, Sørlandet og Vestlandet: Eirik Førland, Jostein Mamen, Karianne Ødemark, Hanne Heiberg, Steinar Myrabø
- Nr. 4 Naturfareprosjektet: Delprosjekt 7. Skred og flomsikring. Sikringstiltak mot skred og flom Befaring i Troms og Finnmark høst 2013
- Nr. 5 Kontrollstasjon: NVEs anbefalinger til endringer i elsertifikatordningen
- Nr. 6 New version (v.1.1.1) of the seNorge snow model and snow maps for Norway. Tuomo Saloranta



Norges
vassdrags- og
energidirektorat

Norges vassdrags- og energidirektorat

Middelthunsgate 29
Postboks 5091 Majorstuen
0301 Oslo

Telefon: 09575
Internett: www.nve.no

